AIAA JOURNAL
Vol. 39, No. 8, August 2001

# Broadband Time-Domain Impedance Models

K.-Y. Fung* and Hongbin Ju†
*Hong Kong Polytechnic University, Kowloon, Hong Kong, People's Republic of China*

**The modeling of a set of impedance values given either experimentally or heuristically for implementation as a time-domain impedance-equivalent boundary condition (TDIBC) is discussed. It is shown that impedance as defined by the reflection of plane harmonic waves when extended for broadband time-domain applications can correspond to mathematically feasible but physically unacceptable noncausal reflection processes. Given a set of impedance data on a finite, positive, and real frequency range, it is possible to construct causal time-domain models that render efficient implementation of TDIBC for broadband reflections. However, these models defined by measurement of harmonic waves may not be valid for the reflection of impulses, for which measurement of transient reflections is warranted.**

## Introduction

IMPEDANCE, defined in the frequency domain as the ratio of pressure and its induced velocity, $Z(\omega) = \hat{p}(\omega)/\hat{u}(\omega)$, has been a well-accepted concept for the reflection of harmonic waves at soft walls. Here $Z$ is the specific impedance, $\hat{p}$ has been normalized by $\rho_0 C_0^2$ the product of free air density $\rho_0$ and sound speed $C_0$, $\hat{u}$ by $C_0$, and the caret denotes Fourier components with $e^{i\omega t}$ time dependence. The characterization of a reflective surface, or the determination of $Z$, relies principally on various comparisons between measured and predicted reflections. Implicit in the definition is the assumption of plane harmonic waves, which are physically difficult to generate. For instance, the standard and widely accepted impedance tube relies on the wall confinement and tube length to establish a train of one-dimensional incident and reflected standing waves through which the complex-valued reflection coefficient, or impedance, is defined when cross-sectional uniformity and harmonic equilibrium are attained. One-dimensionality breaks down when the wavelength of the testing wave is comparable to the tube diameter, or the length of the tube is too short to allow the development of plane waves in the tube for reliable measurement. A broader definition would involve source-to-wall incident-angle dependence, which is often ignored because of many difficulties in broadband characterization of a reflective surface. The impedance tube is only capable of measuring normal reflections, and its use is strictly for locally reactive materials, impedance. A brief survey on the theories and methods for impedance definition can be found in Fung et al.[1]

In principle, the impedance of a surface is defined by the waves it reflects. A finite-time history of the reflected waves measured on any hemispherical surface centered about the point of normal incidence should contain the same information about the reflective surface including angular dependency regardless of the radius of the hemisphere. In practice, the properties of an acoustic absorber are rarely verified in situ after its installation. The difficulties are twofold: the generation of plane harmonic waves for comparing with classical theories and the absence of a practical prediction method for the reflection of physically realizable sources. These difficulties would be alleviated upon the availability of a theory that can correlate in close range and short duration the reference source, the surface to be characterized, and the receptor of the reflected waves. This theory must not be restricted to harmonic waves. It must be phase-time accurate for general broadband waveforms and impedance values and applicable to initial-boundary-value problems. The reflection of a broadband, short-duration acoustic impulse from a general impedance plane should be an ideal setting for experimental testing, but no classical theory has provided a general solution for comparison with such an experiment.

Recent developments in computational aeroacoustics (CAA) have provided a foundation for the development of new theories and testing techniques. However, the treatment of physically meaningful boundary conditions on realistic surfaces, including the treatment of numerical surfaces caused by domain truncation, has been a critical issue in these developments. The objective of this paper is to explore the ways a reflective surface can be suitably characterized for incorporation with CAA for prediction of wave fields in general and broadband reflections in particular.

It has been shown in Fung et al.[1] that the corresponding reflection process to a typical impedance model is a convolution of the incident waves and the reflection impulse. The latter is the inverse Fourier transform of the reflection coefficient, which is related bilinearly to the impedance and often known only as a set of discrete values measured for a range of frequencies. These values do not necessarily have any requirement of continuity because $\omega$ is regarded as a parameter in the solution of the boundary-value problem in classical frequency-domain applications, whereas the inverse Fourier transform process must assume an analytic form to invoke Cauchy's residue theorem. Here we will first address the issues in extending the concept of impedance to a time-domain theory for the reflection of waves.

It will be shown here that the way impedance is extended to cover a broad frequency range has significant implications on the implementation and even validity of the time-domain impedance-equivalent boundary condition (TDIBC). Some extensions may correspond to noncausal and therefore physically unacceptable reflection processes. Indeed, we will show here many common models are noncausal despite their acceptance for solution in frequency domain. Nonetheless, we will propose and demonstrate mathematically stable methods to deal with the physically unacceptable but mathematically feasible solution process. Some forms are preferred, in particular as a set of harmonic oscillators. We will then propose a method for construction of causal reflection models by combinations of harmonic oscillators. This method provides more flexibility in fitting a given set of measured impedance data than polynomial expressions and renders a simple, efficient, recursive algorithm for the implementation of TDIBC.

Although various models can give the same reflection for harmonic waves over finite frequency ranges, we will show that the harmonic assumption implicit in the measurement of impedance values can lead to noncausal and band-restricted models not suitable for reflection of impulses and that the true transient reflection of impulses can require measurement of transient waves rather than the classical measurement of harmonic waves in order to establish causal broadband models for their prediction. The theory to be presented here can be used to better characterize an impedance surface for studies of broadband reflection.

Received 11 March 2000; revision received 23 February 2001; accepted for publication 23 February 2001. 

*Professor, Department of Mechanical Engineering, Hung Hom; mmky fung@polyu.edu.hk. Associate Fellow AIAA.

†Research Fellow, Department of Mechanical Engineering, Hung Hom. Member AIAA.

## Time-Domain Reflection Impulses

We begin with the time-domain reflection process [Eq. (9), Ref. 1], which relates the incident wave $u^+$ to the reflected wave $u^-$ at the right boundary point $x_b$ as

$$u^-(x_b,t)=\int_{-\infty}^{\infty}W(\tau)u^+(x_b,t-\tau)\,\mathrm{d}\tau$$
$$=\int_0^{\infty}W^+(\tau)u^+(x_b,t-\tau)\,\mathrm{d}\tau+\int_{-\infty}^{0}W^-(\tau)u^+(x_b,t-\tau)\,\mathrm{d}\tau \tag{1}$$

Here the reflection function $W(\tau)$ is the Fourier inverse transform of the reflection coefficient $\hat{W}(\omega)\equiv(1-Z)/(1+Z)$, and when expressed in an algebraic function of $\omega$ can assume the form

$$W(\tau)=\begin{cases}W^+(\tau)=i\displaystyle\sum_{\mathrm{Im}(\lambda_k)>0}\mathrm{residue}[\hat{W}(\omega),\lambda_k]e^{i\lambda_k\tau}, & \tau\geq 0\\ W^-(\tau)=-i\displaystyle\sum_{\mathrm{Im}(\lambda_k)<0}\mathrm{residue}[\hat{W}(\omega),\lambda_k]e^{i\lambda_k\tau}, & \tau<0\end{cases} \tag{2}$$

where $\lambda_k$ is the $k$th root of $1+Z(\omega)=0$. The decaying and impulsive characteristics of the reflection coefficient are ensured by the factor $e^{i\lambda_k\tau}$ when none of the roots is purely real. Equations (1) and (2) reveal problems with the classical definition of impedance $Z$, which is defined and measured for plane harmonic waves at discrete real values of $\omega$. The inversion in Eq. (2) assumes analytic continuation of $\hat{W}(\omega)$ to the entire complex $\omega$ plane. If the extension results in poles with negative imaginary parts $\mathrm{Im}(\lambda_k)<0$, the corresponding reflection impulse $W(\tau)$ has an noncausal component in that the evaluation of Eq. (1) involves future incident waves:

$$\int_{-\infty}^{0}W^-(\tau)u^+(x_b,t-\tau)\,\mathrm{d}\tau$$

which is physically unacceptable. This deficiency of the classical frequency-domain approach had been noted in Gilbert et al.[2] and was later explained and treated in Agulló et al.,[3] who derived corresponding impulse responses and time-domain "input reflection functions" of anechoic bores. We will show later that many common impedance models do not necessarily lead to a causal reflection process. Nonetheless, using the space-time equivalence of the incident wave moving at nondimensional sound speed of unity toward a right boundary at $x_b$, e.g., $u^+(x,t)=u^+(x-t)$, Eq. (1) can assume the spatial form ($\Delta t$, a positive time difference)

$$u^-(x_b,t)=\int_0^{T_U}W^+(x)u^+(x_b+x,t)\,\mathrm{d}x$$
$$+\int_{T_L}^{0}W^-(x)u^+(x_b+x-\Delta t,t-\Delta t)\,\mathrm{d}x \tag{3}$$

which can be evaluated for the causal (first) integral with an extended set of values beyond the physical domain boundaries[1] and for the noncausal (second) integral from points in the interior. Here the upper and lower integration limits have been reduced from infinity to $T_U$ and $T_L$, respectively, which depend on the exponential decays of $W(\tau)$ and can be set conveniently as $|\ln\varepsilon/\mathrm{Im}(\lambda_k)|$ for an acceptable integration error bound $\varepsilon$.

The reflection coefficient $\hat{W}(\omega)$ can also be expanded into the polynomial

$$\hat{W}(\omega)=U(\omega)+iV(\omega)=U_0+U_2\omega^2+\cdots+i\left(V_1\omega+V_3\omega^3+\cdots\right) \tag{4}$$

or through a direct exchange of $i\omega$ with $\partial/\partial t$ assume the time-domain differential form for harmonic waves:

$$u^-=\hat{W}\left(\frac{\partial}{i\partial t}\right)u^+=\hat{W}\left(i\frac{\partial}{\partial x}\right)u^+\approx\sum_{k=0}^{n}\frac{(-1)^k}{k!}$$
$$\times\left[\frac{\mathrm{d}^k\bar{U}(\bar{\omega}_0)}{\mathrm{d}\bar{\omega}^k}+\frac{\mathrm{d}^k\bar{V}(\bar{\omega}_0)}{\mathrm{d}\bar{\omega}^k}\frac{\partial}{\partial t}\right]\left(\frac{\partial^2}{\partial t^2}+\omega_0^2\right)^k u^+ \tag{5}$$

where $\bar{U}(\bar{\omega})=U(\omega)$ and $\bar{V}(\bar{\omega})=V(\omega)/\omega$ are all functions of $\bar{\omega}=\omega^2$. Although the differential approach can involve a set of temporal values of $u^+(x_b,t-j\Delta t)$ or spatial values of $u^+(x_b+j\Delta x,t)$ and be considered causal if the values are taken forward in space or backward in time, it is fundamentally a harmonic approach restricted to a range of frequencies about $\omega_0$.

## Broadband TDIBC Schemes

Aside from the causality issue, which will be addressed later, the choice among the various forms of Eqs. (1), (3), or (5) can be based on solution accuracy and algorithmic efficiency. The differential form, Eq. (5), can be the easiest to implement for a given set of impedance data, but is in general not suitable for long-time computation for the growth of spurious waves of frequencies beyond the finite application range of an approximated formula.[1] Furthermore, it restricts the applications to harmonic waves (by the replacement of $i\omega$ with $\partial/\partial t$) and may not be suitable for transient reflections; this will be exemplified later. The integral form poses two problems: finding the roots of $1+Z=0$ and dealing with the negative imaginary roots, or noncausal implementation. The former is a classical problem of applied mathematics, for which various numerical schemes are available. The latter has not been dealt with in the literature perhaps for its apparent violation of causality. If the temporal approach Eq. (1) is taken, only causal roots can be implemented. If causality is disregarded in a temporal approach, instability will result for the violation of the domain of dependence implicit in the characteristics of the solution system. The difficult task of finding an analytic expression for $Z$ that satisfies a set of constraints and ensures roots with positive imaginary parts must be overcome. If the spatial approach Eq. (3) is taken, the integration can be extended spatially toward the incident waves, but the principal direction of the incident wave may be difficult to identify except in one dimension. Noncausal spatial approach is numerically most efficient because it requires no storage of past history, whereas causal temporal or spatial approach requires, respectively, the storage of $T_u/\Delta t$ or $T_u/\Delta x$.

Finding the roots and thus casting $W(\tau)$ in the form of Eq. (2) gives a distinct advantage for implementation. The requirement that the total reflection be a real quantity implies that only purely real or conjugate pairs of $\mu_k e^{i\lambda_k t}$ are acceptable choices. Each of the roots corresponds to the reflection impulse $\mu_k e^{i\lambda_k t}H(t)$, which is always bounded. Here, $H(t)$ denotes the Heaviside function. Assuming causal roots, Eq. (1) takes the form

$$u^-(x_b,t)=\sum_k u_k^-(x_b,t)$$

where

$$u_k^-(x_b,t)=\mu_k\int_0^{\infty}e^{i\lambda_k\tau}u^+(x_b,t-\tau)\,\mathrm{d}\tau$$

which can be approximated using the trapezoidal rule and efficiently implemented with $z_k=e^{i\lambda_k\Delta t}$ in the recursive formula:

$$u_k^-(x_b,t)=\mu_k u^+(x_b,t)\frac{\Delta t}{2}+\mu_k\sum_{j=1}^{\infty}z_k{}^j u^+(x_b,t-j\Delta t)\Delta t$$
$$=\mu_k\left[u^+(x_b,t)+z_k u^+(x_b,t-\Delta t)\right]\frac{\Delta t}{2}+z_k u_k^-(x_b,t-\Delta t)$$

This shows, for the first time, a way to advance by one $\Delta t$ at a time an initial-impedance-boundary-value problem indefinitely without having to localize the infinite integral by truncation and store a set of past history, proportional to $T_u/\Delta t$, as proposed in Ref. 1. For the noncausal roots $\mu_k e^{i\lambda_k t}H(-t)$, a spatial form similar to the second integral of Eq. (3) can be implemented. Thus, noncausal reflection models can be dealt with mathematically regardless of their physical invalidity. Higher-order-accurate recursive formulas can be derived by storage of the repeated integration patterns, such as the two integrals for the odd and even points [1 4 2 4 2 4...] of the Simpson's rule.

## Algebraic Reflection Models

We now consider some common impedance models in the convenient algebraic forms of $\hat{W}(\omega)=\tilde{W}(\omega)-1$, where $\tilde{W}(\omega)=$

$2/(1+Z) = 2/[1+R(\omega^2)+i\omega X(\omega^2)] = Q(s)/D(s)$ for real $R$ and $X$, $s = i\omega$, $D(s) = (s-\lambda_1)(s-\lambda_2)\cdots(s-\lambda_m)$, and thus

$$\hat{\tilde{W}}(\omega) = \Sigma_{k=1}^{m} \hat{\tilde{W}}_k(\omega)$$

with $\hat{\tilde{W}}_k(\omega) = A_k/(s-\lambda_k)$ and $A_k = Q(\lambda_k)/[\mathrm{d}D(\lambda_k)/\mathrm{d}s]$. Because $D(s)$ has only real coefficients, its zeros $\lambda_k$ are either real or complex conjugate pairs.

**Reflection Type-I**

For real $\lambda_k$ the time-domain reflection impulse, denoted as Reflection Type-I,

$$\tilde{W}_k(t) = \begin{cases} A_k e^{\lambda_k t} H(t), & \lambda_k < 0 \\ -A_k e^{\lambda_k t} H(-t), & \lambda_k \geq 0 \end{cases} \tag{6}$$

corresponds to an overly damped system without oscillation, noncausal if $\lambda_k \geq 0$ and causal if $\lambda_k < 0$. An example of this type is the impedance model of the open end of a pipe (Ref. 4, p. 384):

$$Z(\omega) = 1 - \frac{2J_1(\omega)}{\omega} + M(\omega)i$$

$$M(\omega) = \frac{4}{\pi}\int_0^{\pi/2} \sin(\omega\,\cos x)\sin^2 x\,\mathrm{d}x \tag{7}$$

where $J_1$ is the Bessel function of the first kind and $\omega$ has been nondimensionalized by the sound speed $C_0$ and pipe diameter $d$. Analytic inversion of Eq. (7) for $W(t)$ is formidable. Its approximation for low frequencies ($\omega < 1$) is

$$Z = R_2\omega^2 + iX_1\omega \quad \text{with} \quad R_2 = \tfrac{1}{8}, \qquad X_1 = 4/(3\pi) \tag{8}$$

and for high frequencies ($\omega > 10$) is

$$Z = R_0 + iX_{-1}/\omega \quad \text{with} \quad R_0 = 1, \qquad X_{-1} = 4/\pi \tag{9}$$

The low-frequency model equation (8) extended for all frequencies corresponds to the zeros:

$$\lambda_{1,2} = X_1/2R_2 \mp \sqrt{(X_1/2R_2)^2 + 1/R_2}$$

and the reflection impulse

$$W(t) = -\delta(t) + \begin{cases} e^{\lambda_1 t}\Big/\sqrt{R_2 + X_1^2/4}, & t \geq 0 \\ e^{\lambda_2 t}\Big/\sqrt{R_2 + X_1^2/4}, & t < 0 \end{cases} \tag{10}$$

Similarly, the extended high-frequency model Eq. (9) corresponds to

$$W(t) = -(1-R_0)/(1+R_0)\delta(t) - 2X_{-1}\exp[X_{-1}t/(1+R_0)]H(-t) \tag{11}$$

Both extended models Eqs. (10) and (11) involve noncausal processes.

For repeated roots $\lambda_k$ of order $n$, the corresponding impulse response has the form

$$\tilde{W}_k(t) = \begin{cases} A_k t^{n-1} e^{\lambda_k t} H(t)/(n-1)!, & \lambda_k < 0 \\ A_k (-t)^{n-1} e^{\lambda_k t} H(-t)/(n-1)!, & \lambda_k \geq 0 \end{cases}$$

**Reflection Type-II**

When one of the roots $\lambda_k$ of $D(s)$ is complex, its conjugate $\lambda_{k+1}$ must exist to form the pair:

$$\hat{\tilde{W}}_{(k,k+1)}(\omega) \equiv \hat{\tilde{W}}_k(\omega) + \hat{\tilde{W}}_{k+1}(\omega)$$

$$= \frac{A_k}{s-\lambda_k} + \frac{A_{k+1}}{s-\lambda_{k+1}} = \frac{Bs+C}{(s+\alpha)^2+\beta^2} \tag{12}$$

which corresponds to causal or noncausal reflection impulse depending on the sign of $\alpha$:

$$\tilde{W}_{(k,k+1)}(t) =$$

$$\begin{cases} e^{-\alpha t}H(t)[B\,\cos(\beta t) + \dfrac{C-\alpha B}{\beta}\sin(\beta t)], & \alpha \geq 0 \\ -e^{-\alpha t}H(-t)[B\,\cos(\beta t) + \dfrac{C-\alpha B}{\beta}\sin(\beta t)], & \alpha < 0 \end{cases} \tag{13}$$

An example of this reflection type is the response of a damped harmonic oscillator of impedance $Z = R_0 + i(X_1\omega - X_{-1}/\omega)$ with resistance $R_0$, acoustic mass $X_1 = 2/B$, stiffness $X_{-1}$, damping rate $\alpha = (1+R_0)/2X_1$, oscillation frequency $\beta = \sqrt{(\omega_0^2 - \alpha^2)}$, natural frequency $\omega_0 = \sqrt{(X_{-1}/X_1)}$, and an arbitrary phase parameter $C$.

Many sound absorbers are of this three-parameter type, which was used by Botteldooren,[5] Tam and Auriault,[6] and Fung et al.[1] to exemplify their constructions of TDIBC.

## Construction of TDIBC Models

The expression of $W(t)$ hinges on the identification of the roots of $(1+Z)$ or $D(s)$. In practice a set of $Z_j$, or $\hat{\tilde{W}}_j$, are known at discrete frequencies $\omega_j$. A polynomial representation of the data will give the same number of roots as the order of approximation, but the identification of polynomial roots is numerically difficult, and noncausal roots with $\mathrm{Real}(s_j) > 0$ cannot be excluded in general. Here we assume the roots are known and use the convenient forms to construct various impedance models.

We may first assume the Reflection Type-I [Eq. (6)] form

$$\hat{\tilde{W}}(\omega) = \sum_{k=1}^{2L} \frac{A_k}{s-\lambda_k} \tag{14}$$

and arbitrarily choose 12 real roots, $\lambda_k = -k$, $k = 1 \sim 12$, for the set of six measured values, Table 1, of the ceramic tubular liner used in Özyörük et al.[7] The corresponding curves are shown in Fig. 1, and the fitted coefficients are listed here: $A_1$, 68.108774; $A_2$, $-2.133922\times10^4$; $A_3$, $1.739126\times10^6$; $A_4$, $-5.591238\times10^7$; $A_5$, $8.464164\times10^8$; $A_6$, $-6.806680\times10^9$; $A_7$, $3.144497\times10^{10}$; $A_8$, $-8.721191\times10^{10}$; $A_9$, $1.471021\times10^{11}$; $A_{10}$, $-1.473597\times10^{11}$; $A_{11}$, $8.043622\times10^{10}$; and $A_{12}$, $-1.839797\times10^{10}$.

The basis functions used are most sensitive near their poles but become asymptotically similar far away, resulting in the inversion of nearly singular determinant and extremely sparse coefficients $A_k$ unsuitable for computation. If the poles are chosen within the frequency range, the fitted curve will have large undesirable fluctuations between data points. The dashed line in Fig. 1 is an algebraic model of $Z$ cast in the form of a rational polynomial: Eq. (15) of Ref. 7, which in general does not guarantee causal roots and when treated as a differential system will lead to algorithmic instability, as reported in Ref. 7.

Physically it is more appropriate to model sound absorbing material as a set of damped harmonic oscillators, Reflection Type-II [Eq. (12)], in the convenient form

$$\hat{\tilde{W}}(\omega) = \sum_{k=1}^{L} \frac{iA_{2k-1}\omega + A_{2k}}{(i\omega + \tilde{\alpha}\omega_{0k})^2 + \omega_{0k}^2(1-\tilde{\alpha}^2)} \tag{15}$$

This form has been used to model the vibration of structures[8] for which the natural frequencies $\omega_{0k}$ are experimentally determined

**Table 1 Impedance data of a constant depth ceramic tubular liner[7]**

| Frequency, kHz | Impedance |
|---|---|
| 0.5 | 0.41−1.56$i$ |
| 1.0 | 0.46+0.03$i$ |
| 1.5 | 1.08+1.38$i$ |
| 2.0 | 4.99+0.25$i$ |
| 2.5 | 1.26−1.53$i$ |
| 3.0 | 0.69−0.24$i$ |

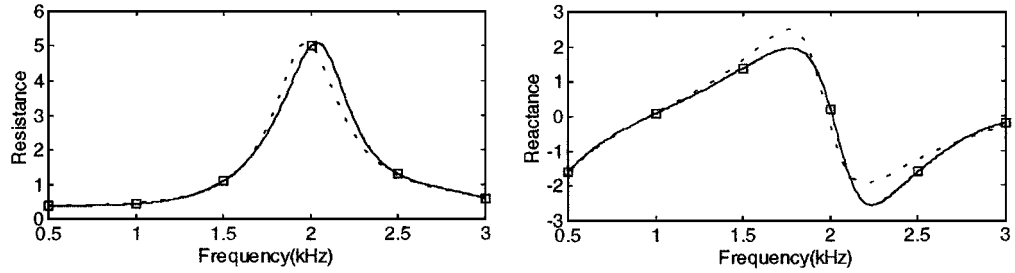


**Fig. 1 Fitted impedance models: □, fitted data; ——, model of Eq. (14); and – – –, Ref. 7.**

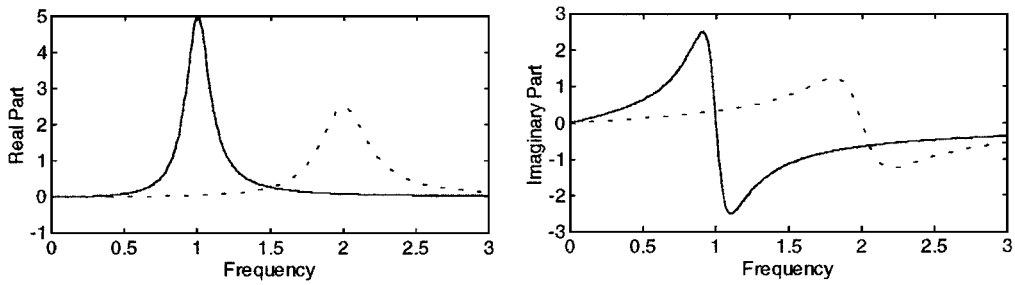


**Fig. 2 Samples of $i\omega/[(i\omega + \bar{\alpha}\omega_0)^2 + \omega_0^2(1 - \bar{\alpha}^2)]$ with ——, $\omega_0 = 1$, $\bar{\alpha} = 0.1$; and – – –, $\omega_0 = 2$, $\bar{\alpha} = 0.1$.**

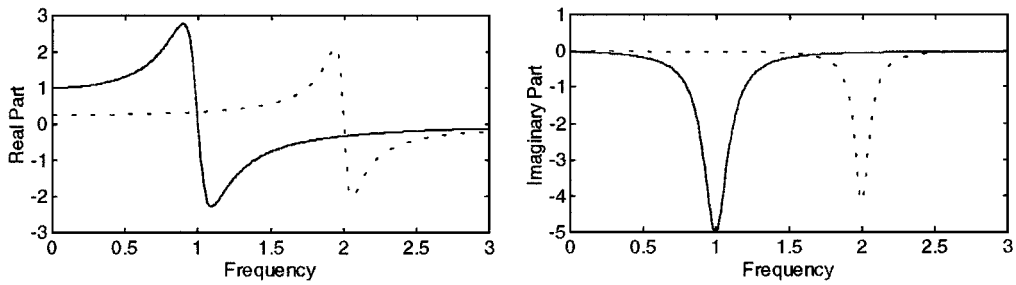


**Fig. 3 Samples of $1/[(i\omega + \bar{\alpha}\omega_0)^2 + \omega_0^2(1 - \bar{\alpha}^2)]$, with ——, $\omega_0 = 1$, $\bar{\alpha} = 0.1$; and – – –, $\omega_0 = 2$, $\bar{\alpha} = 0.03$.**

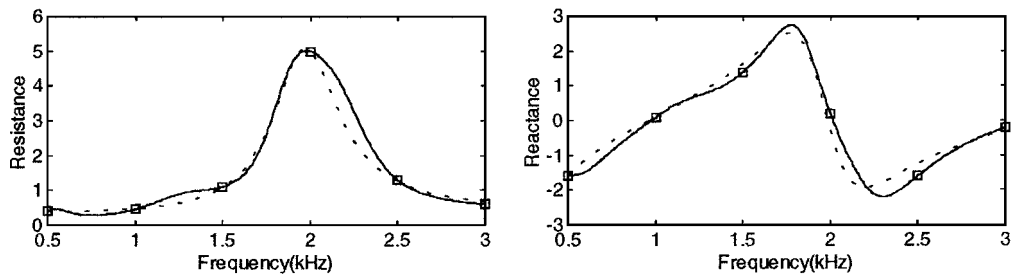


**Fig. 4 Fitted impedance models: □, measured; ——, Eq. (15) with $\omega_{0k} = 0.5, 1, 1.5, 2, 2.5, 3$ kHz, and $\bar{\alpha} = 0.35$; and – – –, Ref. 7.**

and the coefficients $A_k$ and damping $\bar{\alpha}$ are fitted to a set of vibration tests. Because our purpose here is to fit a range of impedance values, $\omega_{0k}$ and $\bar{\alpha}$ need not be physically accurate as long as they are mathematically acceptable. Typical variations of the basis functions in Eq. (15) are shown in Figs. 2 and 3, from which one learns that $\omega_0$ determines the peaks and zeros of the basis functions and $\bar{\alpha}$ determines their smoothness. A distinct set of $\omega_0$ form a linearly independent basis, and the choice of suitable $\bar{\alpha}$ renders smooth variation between given data points. For the same impedance data in Table 1, the choice of the fitted frequencies as $\omega_{0k}$ $(k = 1 \sim 6)$ for Eq. (15) leads to the fitted curves shown in Fig. 4 and the coefficients listed here: $A_1$, 0.22410917069; $A_2$, 0.06991210521; $A_3$, 1.47071621643; $A_4$, 1.04587028108; $A_5$, 2.71210253380; $A_6$, 1.73874204347; $A_7$, 2.01133435955; $A_8$, −6.23497398731; $A_9$, −5.83571839347; $A_{10}$, −8.71073574944; $A_{11}$, 3.30816950948; and $A_{12}$, 4.48607496046. The coefficients are having similar magnitudes and therefore numerically suitable for implementation. The fitted curves are compared with the nonlinear model of Özyörük et al.,[7] a rational polynomial with widely disparate coefficients (Appendix in Ref. 7) for which an iterative procedure is required and stable implementation in their proposed differential form is not guaranteed.[7] The linear models here require a simple matrix inversion for coefficient determination. The small oscillations in the point-by-point-fitted curves can be avoided if lower polynomials are used for lease-squares-fitted curves. Figure 5 shows the fitted curves and listed here are the corresponding coefficients ($A_1$, 1.90600497153; $A_2$, 1.01008285202; $A_3$, 3.01696250912; $A_4$, −6.6478565790) for the same data set using only two values of $\omega_{0k}$ (1.1 and 3.1) and $\bar{\alpha} = 0.45$.

Another practical example is the impedance model for typical outdoor grounds[9]:

$$Z = 0.436(1-i)(38/\omega)^{0.5} - 0.2922i/\omega \qquad (\text{with } \omega \text{ in kHZ}) \quad (16)$$

which can be approximated using three Reflection Type-II oscillators (with $\omega_{0k}$ at 0.2, 1.5, 6 kHz and $\bar{\alpha} = 0.85$, and the $A_k$ listed here: $A_1$, 0.00167401789; $A_2$, −0.0037205512; $A_3$, 1.05956567463; $A_4$, 0.72188743787; $A_5$, 10.1382897393; and $A_6$, −7.62130801470) as shown in Fig. 6. The small coefficient of $A_1$

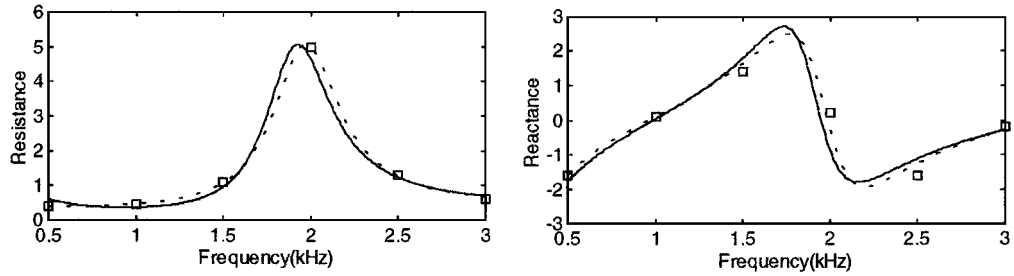


**Fig. 5 Fitted impedance models: □, measured; ——, least-squares fitted model with $\omega_{0k} = 1.1, 3.1$ kHz, and $\bar{\alpha} = 0.45$; and – – –, Ref. 7.**

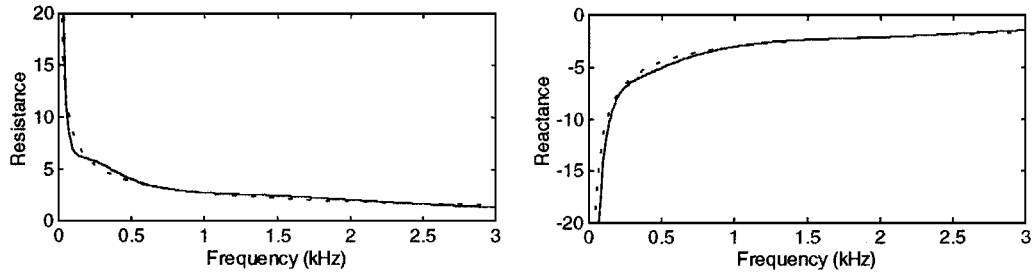


**Fig. 6 Fitted impedance models: ——, Eq. (15) with $\omega_{0k} = 0.2, 1.5, 6$ kHz, and $\bar{\alpha} = 0.85$; and – – –, analytical model equation (16).**

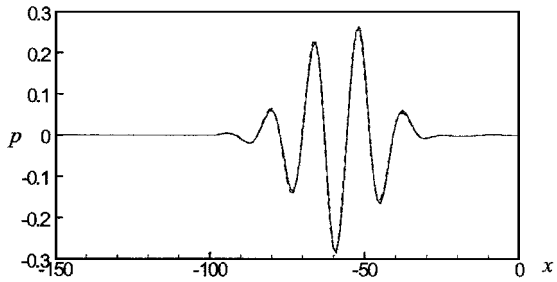


**Fig. 7 Reflected pressure pulses at $t = 150$: ——, numerical, and – – –, analytical with the reflection model of Eq. (15) and coefficients corresponding to Fig. 5.**

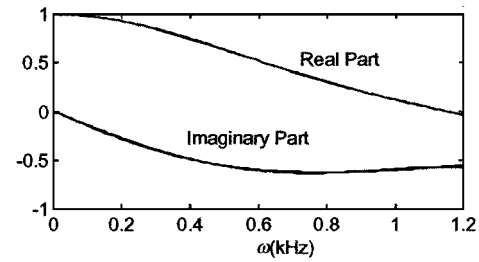


**Fig. 8 Reflection coefficient models for the open end of a pipe of diameter 0.3 m: ——, Eq. (17), and – – –, Eq. (8).**

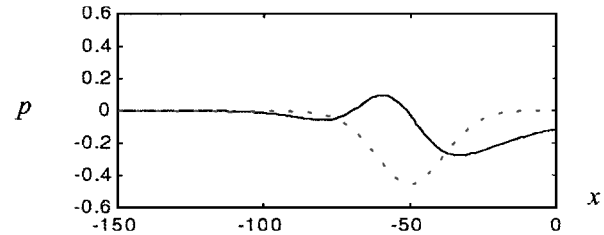


**Fig. 9 Pressure field in an open end pipe at $t = 140$, pipe diameter 0.3 m: ——, TDIBC Eq. (1), and – – –, TDIBC Eq. (5).**

and $A_2$ are for the important contribution of the pole at $\omega_{01} = 0.2$, which may not be ignored.

To verify the composite broadband model Eq. (15), we computed the reflection of the initial pulse: $u(x, 0) = 0$ and $p(x, 0) = \exp[-0.0044(x + 83.333)^2] \cdot \cos[0.444(x + 83.333)]$ of central frequency 2 kHz and bandwidth 1 kHz, in a semi-infinite duct measured in units of 0.012 m from the impedance end at $x = 0$ for the ceramic tubular liner model coefficients corresponding to Fig. 5 implemented with the compact scheme (C3N) of Fung el al.[10] Figure 7 shows the excellent agreement between the computed pressure and the analytical solution.

## TDIBC for Impulses

Implicit in the classical definition of impedance is the assumption of harmonic waves. The time-domain equivalent Eq. (1) does not require specifically this assumption, but the measurement of $\hat{W}$ has so far been from harmonic experiments. A direct way to measure and define the reflection coefficient is the transformed reflected to incident waves ratio $\hat{W} = \hat{u}^-/\hat{u}^+$, which can be measured and computed for compact impulses in an impedance tube and must not have a noncausal component because the resultant reflection $\hat{u}^-$ is experimentally confirmed. Whether this reflection coefficient would agree with $(1 - Z)/(1 + Z)$ from impedance measurement of harmonic waves can only be confirmed experimentally. It is, however, unlikely that the ratio remains the same for all incident waves, but consistency should be found for banded waves or the concept of impedance is unsuitable for the reflection of impulses. We now explore the possible discrepancy and inapplicability of the harmonically measured and mathematically extended impedance for the reflection of impulses.

Equation (8) has been used to model the reflection of low-frequency harmonic waves at the open end of a pipe. This model is mathematically equivalent to the reflection impulse of Eq. (10), which as mentioned earlier involves a noncausal process but can be spatially implemented. For the reflection of the Gaussian pulse $u(x, 0) = 0$ and $p(x, 0) = \exp[-0.0044(x + 83.333)^2]$ of bandwidth [0, 1.2] kHz, in the same duct as earlier, Eq. (8) can be well approximated within the frequency range by the expansion for unit length 0.012 m, whose

$$\hat{W}(\omega) \approx 0.9927 - 1.6864\omega^2 + 1.1442\omega^4 - 0.331\omega^6 + i(-1.3992\omega + 1.2077\omega^3 - 0.3973\omega^5) \tag{17}$$

as the two curves, Eqs. (8) and (17), shown in Fig. 8 practically coincide.

The solid and dashed lines in Fig. 9 represent the different reflections computed using the C3N scheme implemented with Eqs. (1) and (5), respectively. The earlier response shown in the solid line rather than that in the dashed line can be attributed to the noncausal part of the convolution process, which includes the advancing wave values before the impedance at $x = 0$. The much-extended tail of

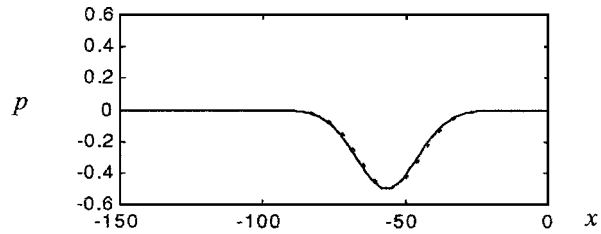


**Fig. 10 Pressure field in an open end pipe at $t = 140$, pipe diameter 0.05 m: ——, TDIBC Eq. (1), and – – –, TDIBC Eq. (5).**

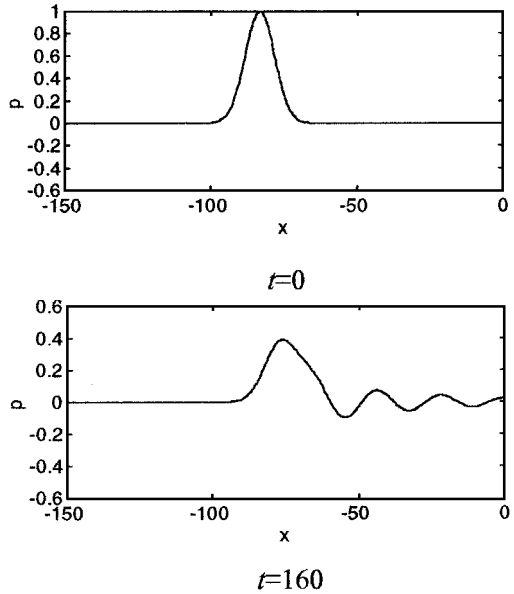


**Fig. 11 Pressure fields with impedance $Z = 0.2 + i(-53.48/\omega + 0.8\omega)$ and computed using integral form equation (1).**

the solid line corresponds to the slow resistive nature of Reflection Type-I, which requires a long duration (proportional to $1/\lambda_1$, i.e., $T_U = 156$ for a pipe diameter of 0.3 m) to establish the harmonic equilibrium state, much longer than the effective pulse duration of 50 time units. The differential form implicitly assumes harmonic equilibrium and uses the local frequency contents to determine the reflection. Figure 10 shows the agreed reflections of using the integral and differential forms for a pipe diameter 0.05 m for which the material response times ($T_L = 12.1$, $T_U = 29.8$) are shorter than the pulse duration. This suggests that when the response time of an impedance wall is longer than the duration of the incident impulse the impedance as defined for plane harmonic waves is invalid and cannot be used to describe the reflection of the impulse. Experimental studies are needed to support the extendibility of the concept of impedance from frequency domain to time domain for acoustic impulses. Because of the locations of the poles in the complex plane, the expansion Eq. (17) has only a radius of convergence of $r_0 = 0.891$ kHz for pipe diameter 0.3 m, much less than the needed range of application.

Similar problems arise for Reflection Type-II impedance near their resonance states. The response of this type of impedance $Z = R_0 + i(X_1\omega - X_{-1}/\omega)$ corresponds physically to that of a damped harmonic oscillator. Figure 11 shows the incident impulse at $t = 0$ and the reflected impulse at $t = 160$ computed with $R_0 = 0.2$, $X_{-1} = 53.48$, $X_1 = 0.8$, and $\omega$ in kiloradian/s. The incident impulse $u(x, 0) = 0$, $p(x, 0) = \exp[-0.02(x + 83.333)^2]$ has an effective pulse width of 30 and frequency range between 0 and 3 kHz. The resonatorlike impedance has the natural frequency $\omega_0 = 1.302$ kHz, which is within the excitation range of the incident wave, but the response time of $T_U = 189$ is much longer than the incident pulse width. The excited response at the natural frequency is clearly shown in the trailing oscillatory tail of the reflected wave, which was computed using the integral approach. The differential approach cannot be used in this case for the expansion about $\omega = 0$ would only have a radius of convergence of $r_0 = 1.302$ kHz much shorter than the desirable range of application.

In a conventional impedance experiment impedance values are taken over finite ranges on the real axis of $\omega$. The extension to time domain according to the theory of Fung et al.[1] requires analytic continuation of $\hat{W}(\omega)$ into the entire complex $\omega$ plane. It is well known in the circuit theory that the transient response of a linear circuit can be described by a set of complex residues, whose identification requires time-limited excitations.[11] It seems that the complex residues of $\hat{W}(\omega)$ can be an effective means for the characterization of a reflective surface, but their location remains illusive for only harmonic excitations have been customarily used.

## Conclusions

We have pointed out some issues concerning the modeling and implementation of TDIBC and demonstrated with practical examples how different types of conventionally defined impedance for harmonic waves can correspond to a set of reflection impulses and assume simple recursive forms for easy efficient numerical implementation. These reflection impulses can be viewed as complex resonances of the reflective wall. For narrowband harmonic applications the identification of these impulses is not critical because only their effect on a short interval of the real frequency axis is needed. The identification of these impulses becomes increasingly important and difficult for applications of broader frequency bands. For transient excitations the impedance measured and defined for harmonic waves can be inadequate to describe the response of the wall as a reflection. Experiments using time-limited excitations and time-domain prediction methods are proposed for better characterization of reflective walls.

## Acknowledgments

Financial support for the second author on PolyU Grant G-YW23 and general support on PolyU Grant G-T053 are acknowledged.

## References

[1]Fung, K.-Y., Ju, H. B., and TallaPragada, B., "Impedance and Its Time-Domain Extensions," *AIAA Journal*, Vol. 38, No. 1, 2000, pp. 30–38.

[2]Gilbert, J., Kergomard, J., and Polack, J. D., "On the Reflection Functions Associated with Discontinuities in Conical Bores," *Journal of the Acoustical Society of America*, Vol. 87, No. 4, 1990, pp. 1773–1780.

[3]Agulló, J., Barjau, A., and Martínez, J., "On the Time-Domain Description of Conical Bores," *Journal of the Acoustical Society of America*, Vol. 91, No. 2, 1992, pp. 1099–1105.

[4]Morse, P. M., and Ingard, K. U., *Theoretical Acoustics*, McGraw-Hill, New York, 1968.

[5]Botteldooren, D., "Finite-Difference Time-Domain Simulation of Low-Frequency Room Acoustic Problems," *Journal of the Acoustical Society of America*, Vol. 98, No. 6, 1995, pp. 3302–3308.

[6]Tam, C. K. W., and Auriault, L., "Time-Domain Impedance Boundary Conditions for Computational Acoustics," *AIAA Journal*, Vol. 34, No. 5, 1996, pp. 917–923.

[7]Özyörük, Y., Long, L. N., and Jones, M. G., "Time-Domain Numerical Simulation of a Flow-Impedance Tube," *Journal of Computational Physics*, Vol. 146, No. 1, 1998, pp. 29–57.

[8]Guan, D. H., *Modal Analysis Techniques*, Tsinghua Univ. Press, Beijing, 1996, p. 53 (in Chinese).

[9]Li, K. M., Taherzadeh, S., and Attenborough, K., "Sound Propagation from a Dipole Source near an Impedance Plane," *Journal of the Acoustical Society of America*, Vol. 101, No. 6, 1997, pp. 3343–3352.

[10]Fung, K.-Y., Man, R. S. O., and Davis, S., "Implicit High-Order Compact Algorithm for Computational Acoustics," *AIAA Journal*, Vol. 34, No. 10, 1996, pp. 2029–2037.

[11]Poggio, A. J., Van Blaricum, M. L., Miller, E. K., and Mittra, R., "Evaluation of a Processing Technique for Transient Data," *IEEE Transactions on Antennas and Propagation*, Vol. AP-26, No. 1, 1978, pp. 165–173.

P. J. Morris
*Associate Editor*